Gene duplication and functional divergence of the zebrafish insulin-like growth factor 1 receptors

Peter J. Schlueter,* Tricia Royer,* Mohamed H. Farah,* Benjamin Laser,* Shu Jin Chan,† Donald F. Steiner,† and Cunming Duan*,[1]

*Department of Molecular, Cellular, and Developmental Biology, University of Michigan, Ann Arbor, Michigan, USA; and †Howard Hughes Medical Institute, University of Chicago, Chicago, Illinois, USA

To read the full text of this article, go to http://www.fasebj.org/cgi/doi/10.1096/fj.05–3882fje

SPECIFIC AIMS

Recent studies have shown that zebrafish have two distinct insulin-like growth factor type 1 receptor (IGF1R) genes, *igf1ra* and *igf1rb*; however, their relationship and their functions are unknown. The aim of this study was to test the hypothesis that zebrafish *igf1ra* and *igf1rb* resulted from a gene duplication event that led to their functional divergence.

PRINCIPAL FINDINGS

1. Genomic structure and chromosomal locations of zebrafish *igf1ra* and *igf1rb*

The zebrafish *igf1ra* spans 151.5 kb in the genome and has 21 exons. The zebrafish *igf1rb* spans 156.5 kb and has 22 exons. Comparisons of exon number and length of the two zebrafish genes with those of the human *IGF1R* gene indicated a high degree of cross-species conservation. *igf1ra* is located on zebrafish linkage group (LG) 18, while *igf1rb* is located on LG 7. Further analysis suggested that *igf1rb* and six other zebrafish genes located on LG 7 have orthologs on human chromosome 15. Similarly, *igf1ra* and four other zebrafish genes located on LG 18 also have orthologs on human chromosome 15. Therefore, the two zebrafish *igf1r*s are encoded by distinct genetic loci believed to evolve from a common ancestral *IGF1R* locus, and there is strong syntenic correspondence between the two zebrafish *igf1r* genes and the human *IGF1R* gene.

2. Both *igf1ra* and *igf1rb* are required for proper zebrafish embryonic growth, development, and survival

To elucidate the functional relationship between *igf1ra* and *igf1rb*, we knocked down each individually or in combination using an antisense MO-based targeted gene knockdown approach. Two distinct antisense MOs were designed for each target gene, and their efficacy and specificity in targeting their respective *igf1r* gene product were validated. Two gene-specific mis-sense MOs were used as controls. Knockdown of *igf1ra* or *igf1rb* resulted in embryos that were smaller and more developmentally delayed than control MO-injected embryos (**Fig. 1*A***). These embryos survived to 48 hpf, and ~50% were alive at 72 hpf but none beyond 96 hpf. At 24 hpf, the mean body length and somite number of *igf1ra* and *igf1rb* MO-injected embryos were significantly reduced (Fig. 1*B, C*). When both *igf1ra* and *igf1rb* were knocked down by injecting a combination of all four targeting *igf1r* MOs, all embryos died by 30 hpf. At 24 hpf, their body size and developmental rate (somite number) were significantly smaller than those of the single knockdown group (Fig. 1*B, C*), suggesting the two genes play similar and likely additive roles in regulating embryonic growth, developmental rate, and survival.

3. Overlapping functions of *igf1ra* and *igf1rb* in regulating embryonic tissue growth and differentiation

To determine the roles of *igf1ra* and *igf1rb* in organogenesis, we analyzed the impact of knocking down *igf1ra* or *igf1rb* on eye, inner ear, and heart formation and differentiation. Knockdown of either *igf1ra* or *igf1rb* caused similar reductions in the expression levels of *rx1* mRNA, a retina-specific homoebox gene. There was also a similar absence of differentiated retinal ganglion cells in the retina and sensory hair cells in the otic vesicles in *igf1ra* and *igf1rb* MO-injected embryos. Knockdown of *igf1ra* or *igf1rb* individually also caused a similar degree of delay in the timing of heart morphogenesis and reduction of differentiated cardiac tissue. These results indicated that *igf1ra* and *igf1rb* play largely similar roles in eye, inner ear, and heart development.

[1] Correspondence: Department of MCDB, University of Michigan, Kraus Natural Science Bldg., Ann Arbor, MI 48109, USA. E-mail: cduan@umich.edu

doi: 10.1096/fj.05-3882fje

0892-6638/06/0020-1230 © FASEB

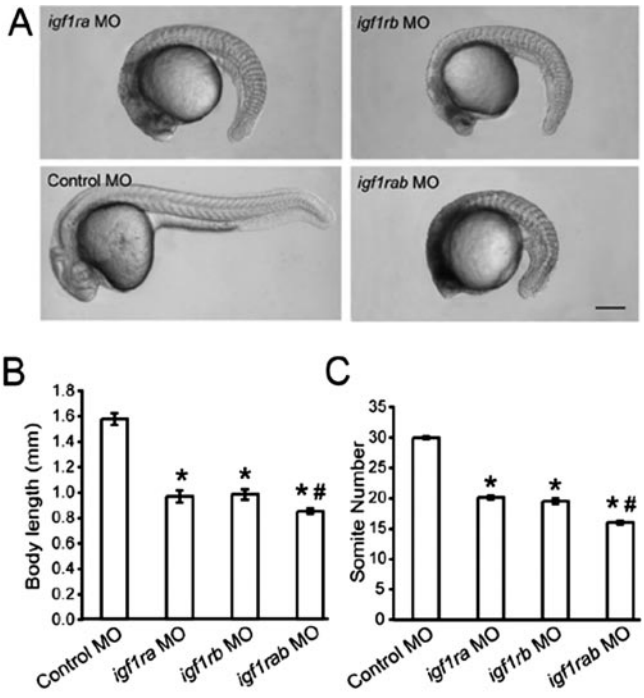

Figure 1. Zebrafish *igf1ra* and *igf1rb* play overlapping but nonredundant roles in regulating growth and developmental rate. *A)* Morphology of 24 hpf embryos injected with *igf1ra* MOs, *igf1rb* MOs, *igf1ra* MOs + *igf1rb* MOs (*igf1ra*b MO), or control MOs. Scale bar = 250 μm. *B)* Body length and *C)* somite number of embryos shown in panel *A*. Results are from 3 independent experiments, each with 15 embryos per group. $*P < 0.0001$ compared with the control MO-injected group, and $\#P < 0.001$ compared with that of the *igf1ra* or *igf1rb* MO-injected group.

4. Igf1rb plays a greater role in spontaneous muscle contractility and motoneuron development

During the course of the study, we noticed a marked difference in spontaneous contractile activity among the experimental groups. Wild-type zebrafish embryos spontaneously contract their tail muscles at 24 hpf as their motoneuron axons innervate the somitic myotome. By 48 hpf, this spontaneous contractility ceases and embryos exhibit rhythmic bouts of swimming. Control MO-injected embryos were indistinguishable from their wild-type siblings, 100% exhibiting spontaneous muscle contractions at 24 hpf and 0% at 48 hpf (**Fig. 2*A***). In the *igf1ra* MO-injected group, 69.0 ± 3.07% of the embryos at 24 hpf and 91.5 ± 0.54% at 48 hpf displayed spontaneous contractility, indicating that depletion of *igf1ra* delayed the timing of this behavior. In contrast, few of the *igf1rb* MO-injected embryos exhibited spontaneous muscle contractility at either 24 hpf (8.65±0.60%) or 48 hpf (5.5±0.75%), suggesting that depletion of *igf1rb* either abolished this behavior or caused a greater delay.

The lack of spontaneous muscle contractility would imply defects in muscle differentiation, motoneuron innervation, or both. Whole mount *in situ* hybridization analysis showed that both *igf1ra* and *igf1rb* MO-injected embryos exhibited robust mRNA expression of *myoD* (Fig. 2*B*, upper panels) and *myogenin* (data not shown) at 24 hpf, indicating normal somitogenesis. F59 staining of fast and slow muscle indicated that knockdown of either *igf1ra* or *igf1rb* caused a reduction in muscle differentiation and the degree of reduction was comparable (Fig. 2*B*, middle panels). Therefore, although muscle differentiation was impaired, it is not likely the underlying cause of the difference observed in spontaneous muscle contractility. These results led us to hypothesize alternately that *igf1rb* may play a greater or more specific role in promoting motoneuron differentiation. This idea was tested by staining embryos with an antibody against SV2, which labels motoneurons and their axons. As shown in Fig. 2*B*, axons from the caudal primary motoneurons (CaP) of control MO-injected

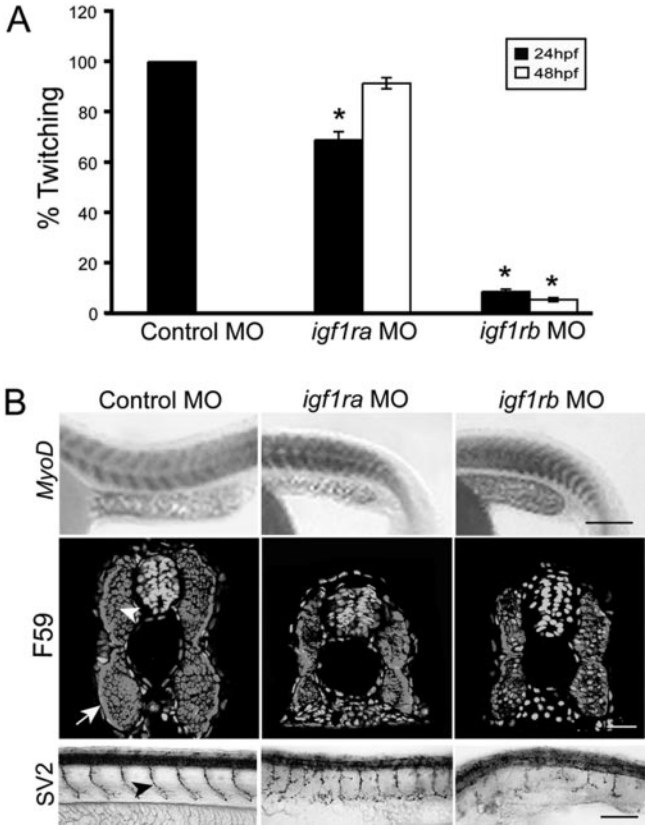

Figure 2. Igf1rb plays a greater role in regulating spontaneous muscle contractility and motoneuron differentiation. *A)* Percent of embryos exhibiting spontaneous muscle contractility at 24 (filled bar) or 48 hpf (open bar) in the control, *igf1ra,* or *igf1rb* MO-injected group. Results were obtained from 3 independent microinjection experiments, with 45 embryos per group. $*P < 0.0001$. *B)* Expression pattern of *myoD* mRNA in 24 hpf control, *igf1ra,* or *igf1rb* MO-injected embryos (upper panel). Scale bar = 250 μm. Slow and fast muscle muscles (labeled by F59 staining, red) in 48 hpf control, *igf1ra,* or *igf1rb* MO-injected embryos (middle panel). The sections were counterstained with sytox (green, nuclear staining). Scale bar = 20 μm. CaP motoneuron axons (labeled by SV2 staining, dark) in 48 hpf control, *igf1ra*, and *igf1rb* MO-injected embryos (bottom panel). Scale bar = 100 μm. Lateral views are shown with anterior to the left and dorsal up.

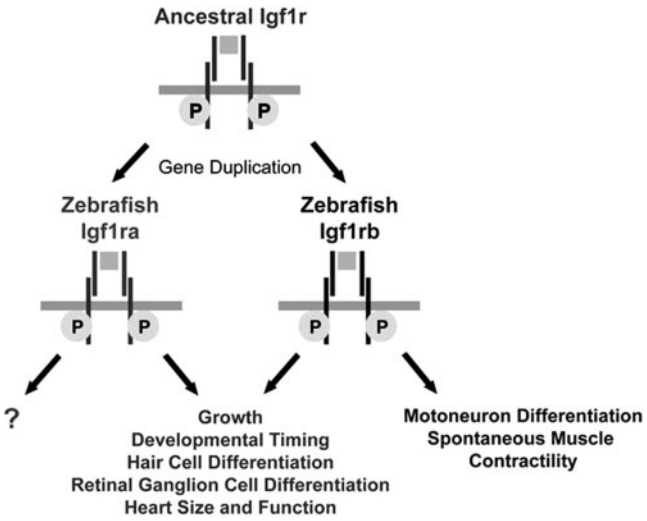

Figure 3. A schematic diagram illustrating the duplication and subsequent functional diversification of zebrafish *igf1ra* and *igf1rb*.

embryos clearly innervated the muscle and were well organized; however, CaP axons in *igf1ra* and *igf1rb* MO-injected embryos were significantly impaired, but the effect was more pronounced in the *igf1rb* MO-injected embryos. The *igf1rb* MO-injected embryos had 4.5 ± 0.46 CaP axons, significantly less than the 8.4 ± 0.8 axons in *igf1ra* MO-injected embryos, and the 9.0 ± 0.0 axons in control MO-injected embryos ($p < 0.0001$). These data suggest that while both Igf1ra and Igf1rb are important for muscle differentiation, Igf1rb plays a greater or more specific role in promoting motoneuron innervation.

CONCLUSIONS AND SIGNIFICANCE

In this study we provide evidence that zebrafish Igf1ra and Igf1rb are encoded by two distinct genetic loci believed to have evolved from a common ancestral locus. Additionally, we show a strong syntenic correspondence between the two zebrafish *igf1r* genes and the human *IGF1R* gene, suggesting that zebrafish *igf1ra* and *igf1rb* likely originated from a gene duplication event that occurred during teleost evolution. This conclusion is consistent with the notion that zebrafish and other fishes in the killifish lineage may have experienced an additional gene duplication event during evolution, a theory derived from studies of the Hox gene family in zebrafish and *Fugu*.

Gene duplication is thought to be the primary source of new genes. Permanent preservation of both duplicates requires divergent functions, but deciphering whether a pair of duplicated genes has evolved divergent functions is often challenging. In this study, we explored the power of the zebrafish model and determined the functional relationship of the duplicated zebrafish *igf1r* genes. Knockdown of zebrafish *igf1ra* and *igf1rb* together resulted in 100% lethality by 30 hpf. These embryos were significantly smaller, about half that of their wild-type siblings, and exhibited significantly reduced somite number, suggesting developmental delay. These phenotypes are consistent with those reported in human patients and *Igf1r* null mice. When a single *igf1r*, either *igf1ra* or *igf1rb* was knocked down, the embryos could survive beyond 48 hpf, but with greatly increased mortality rates thereafter. Knockdown of *igf1ra* or *igf1rb* individually resulted in similar reductions in body size, development rate, differentiated RGCs, sensory hair cells in the inner ear, and skeletal muscle. Heart development and growth were also impaired in these embryos. These results suggest that the duplicated zebrafish *igf1r* genes play largely similar roles in zebrafish development.

Despite these apparent overlapping functions, *igf1ra* and *igf1rb* are not strictly redundant but appear to play additive roles, because embryos lacking both receptors are more severely growth and developmentally retarded than embryos lacking either receptor alone. While knockdown of either *igf1rb* or *igf1ra* caused a comparable reduction in muscle differentiation, knockdown of *igf1rb*, but not *igf1ra*, caused a failure of embryos to exhibit spontaneous muscle contractility. Further analysis indicated that Igf1rb plays a greater or more specific role in promoting motoneuron innervation of the myotome. The mechanism underlying the functional differences in spontaneous muscle contractility and motoneuron differentiation between zebrafish Igf1ra and Igf1rb is not yet clear. Differences in ligand binding affinities, gene expression patterns, and/or signal transduction mechanisms may account for the functional specificity of the two zebrafish *igf1r* genes. The two zebrafish Igf1rs are only 70% identical to each other, with the divergent residues spread throughout the molecules, and there are significant differences in their cytoplasmic regions. It is possible that these divergent sequences may confer different signaling capacities between the two receptors. Further studies focusing on determining whether the duplicated zebrafish Igf1rs possess similar or different cellular distribution patterns and/or signaling properties will be needed to elucidate the molecular mechanisms underlying their functions. FJ

Gene duplication and functional divergence of the zebrafish insulin-like growth factor 1 receptors

Peter J. Schlueter[1], Tricia Royer[1], Mohamed H. Farah[1], Benjamin Laser[1], Shu Jin Chan[2], Donald F. Steiner[2], and Cunming Duan[1]

Department of Molecular, Cellular, and Developmental Biology, University of Michigan, Ann Arbor, MI 48109; and Howard Hughes Medical Institute, University of Chicago, Chicago, IL 60637

ABSTRACT **Insulin-like growth factor (IGF) 1 receptor (IGF1R)-mediated signaling plays key roles in growth, development, and physiology. Recent studies have shown that there are two distinct *igf1r* genes in zebrafish, termed *igf1ra* and *igf1rb*. In this study, we tested the hypothesis that zebrafish *igf1ra* and *igf1rb* resulted from a gene duplication event at the *igf1r* locus and that this has led to their functional divergence. The genomic structures of zebrafish *igf1ra* and *igf1rb* were determined and their loci mapped. While zebrafish *igf1ra* has 21 exons and is located on linkage group (LG) 18, zebrafish *igf1rb* has 22 exons and mapped to LG 7. There is a strong syntenic relationship between the two zebrafish genes and the human *IG F1R* gene. Using a MO-based loss-of-function approach, we show that both Igf1ra and Igf1rb are required for zebrafish embryo viability and proper growth and development. Although Igf1ra and Igf1rb demonstrated a large degree of functional overlap with regard to cell differentiation in the developing eye, inner ear, heart, and muscle, they also exhibited functional distinction involving a greater requirement for Igf1rb in spontaneous muscle contractility. These findings suggest that the duplicated zebrafish *igf1r* genes play largely overlapping but not identical functional roles in early development and provide novel insight into the functional evolution of the IGF1R/insulin receptor gene family.—Schlueter, P. J., Royer, T., Mohamed, H. F., Laser, B., Chan, S. J., Steiner, D. F., Duan, C. Gene duplication and functional divergence of the zebrafish insulin-like growth factor 1 receptors. *FASEB J.* 20, E462–E471 (2006)**

Key Words: IGF signaling · growth · developmental timing · retina · inner ear · heart · muscle

THE TYPE-1 IGF receptor (IGF1R), which binds to and is activated by IGF1 or IGF2, plays key roles in human growth, development, and physiology (1–3). The human IGF1R is a heterotetrameric transmembrane protein, consisting of two α and two β subunits, linked by disulfide bonds (4). Ligand binding induces IGF1R autophosphorylation at tyrosine residues, activating multiple downstream signal transduction cascades, including the mitogen-activated protein kinase (MAPK) pathway and phosphoinositide-3-kinase (PI3K)-Akt pathway (1, 2). Patients with point mutations in the *IGF1R* gene exhibited severe intrauterine growth restriction and poor postnatal growth (5, 6). Likewise, loss-of-function mutations in the human *IGF1* gene resulted in severe fetal and postnatal growth failure, and in mental retardation and sensorineural deafness (7–9).

The central role of IGF1R-mediated signaling in growth or size control has been demonstrated by mouse genetic studies. Homozygous *Igf1r* null mutant mice exhibited severe but proportional growth retardation (45% of the wild type littermates) and neonatal lethality (10, 11). Although *Igf1r* knockout mice exhibited decreased numbers of specific neurons and reduced myelination, there was no evidence of major organ loss or patterning abnormalities (10, 11). Therefore, the IGF1R-mediated signaling is believed to be a key growth regulator in development (12, 13). Recent studies in *Xenopus* suggested that IGF1R-mediated signaling is important for anterior neural induction (14–16); similarly, a study using zebrafish reported that overexpression of a similar dominant negative IGF1R construct caused defects in head and central nervous system development (17).

Recently we have shown that there are two distinct *igf1r* genes in zebrafish, termed *igf1ra* and *igf1rb*, and that they are expressed in overlapping spatial domains throughout embryogenesis (18). Like the human IGF1R, both zebrafish Igf1ra and Igf1rb are heterotetrameric transmembrane proteins, consisting of two α and two β subunits, and they bind to IGFs but not to insulin. The relationship between the two zebrafish *igf1r* genes, however, is not clear and their functions are unknown. In this study, we tested the hypothesis that *igf1ra* and *igf1rb* originated from a gene duplication event, which led to their functional divergence. Our results suggest that zebrafish *igf1ra* and *igf1rb* are encoded by distinct genetic loci believed to evolve from a common ancestral gene, and there is strong syntenic correspondence between zebrafish *igf1ra* and *igf1rb*

[1] Correspondence: Department of MCDB, University of Michigan, Kraus Natural Science Bldg., Ann Arbor, MI 48109, USA. E-mail: cduan@umich.edu

doi: 10.1096/fj.05-3882fje

0892-6638/06/0020-0462 © FASEB

and the human *IGF1R* gene. Employing a MO-based targeted gene knockdown approach, we provide evidence that *igf1ra* and *igf1rb* play largely overlapping, but not identical roles in zebrafish development.

MATERIALS AND METHODS

Materials

All chemicals and reagents were purchased from Fisher Scientific (Pittsburgh, PA) unless otherwise noted. RNase-free DNase was purchased from Promega (Madison, WI). Restriction endonucleases were purchased from New England BioLabs (Beverly, MA). PCR primers were synthesized by Invitrogen Life Technologies, Inc. (Carlsbad, CA). Akt antibodies were purchased from Cell Signaling (Beverly, MA), the anti-Tubulin antibody (Ab) was purchased from Sigma (St. Louis, MO), and the SV2 and Zn5 monoclonal antibodies were purchased from the Developmental Studies Hybridoma Bank (University of Iowa). The LN54 radiation hybrid panel was kindly provided by Dr. M. Ekker, and the F59 Ab by Dr. F. Stockdale. Plasmid DNAs for making various riboprobes were generously provided by Drs. R. Kollmar (*claudin-a*), S. Lyons (*nkx2.5*), P. Raymond (*rx1, rx2*) and S.J. Du (*myoD, myogenin*).

Experimental animals

Adult wild-type (WT) zebrafish (*Danio rerio*) were maintained at 28 C on a 14h:10h (light: dark) cycle, and fed twice daily. Embryos were generated from natural crosses. Fertilized eggs were raised in embryo medium at 28.5°C and staged according to Kimmel et al. (19). All experiments were conducted in accordance with guidelines approved by the University Committee on the Use and Care of Animals, University of Michigan.

Determining the structure and physical mapping of zebrafish igf1ra and igf1rb

The zebrafish *igf1ra and igf1rb* genomic structures were determined by searching zebrafish genome (http://www.ensembl.org/Multi/blastview?species=Danio rerio) and PCR. Physical mapping was carried out using the LN54 radiation hybrid panel (20). Primers used for mapping *Igf1ra* amplified the last 197 bp of exon 21 and the first 142bp of the 3′ UTR (forward 5′-CAGGCCTGGCTCTGGATAAGCACTCAG-3′ and reverse 5′-TGCCCAAACCGTCCTCCGTCATTCCAA-3′). Primers used for mapping *Igf1rb* amplified a 222 bp portion of exon 22 (forward 5′-GATGCGTCGGATGTGTGTCAAGCCACT-3′ and reverse 5′- CAGTCAGTGATCCTGTCTGGCGGAAAT-3′).

Morpholino knockdown

MOs were designed according to criteria provided by the commercial supplier (Gene Tools, LLC; Corvallis, OR). Two antisense MOs were designed against distinct sequences in the 5′ UTR of each zebrafish *igf1r*. The two *igf1ra* targeting MOs are: *igf1ra* MO 1, 5′-TCGCTGTTCCAGATCTCATTCCTAA-3′; and *igf1ra* MO 2, 5′-TGAAATTGCAGAAAAACGCGAGGCT -3′. The two *igf1rb* targeting MOs are: *igf1rb* MO 1, 5′-TGTTTGCTAGACCTCATTCCTGTAC-3′; and *igf1rb* MO 2, 5′AGAAATTAGGGAGAGACACCTCAAC-3′. In addition, we used two gene-specific mis-sense control MOs (*igf1ra* Control MO, 5′-TCGgTGTagCAGATCTCtTTCgTAA-3′; and *igf1rb* Control MO, 5′- TGaaTGCaAGAtCTCATaCCTcTAC-3′; small letters indicate nucleotide substitutions).

Construction of the igf1ra- and igf1rb-GFP reporter plasmids

A 650 bp cDNA fragment corresponding to a portion of the 5′ UTR of the zebrafish *igf1ra* gene (including the MO targeting regions) was generated by RT-PCR (forward primer, 5′-TTTTTGTTGGAGGAGAAGCCG-3′; reverse primer, 5′-TTACCATGGTCAACTTGGGGA-3′). The amplified DNA fragment was digested with *Eco*RI and *Pst*I and was then subcloned into the pEGFP-N1 plasmid (Clontech; Palo Alto, CA). Similarly, an 880 bp DNA fragment corresponding to a portion of the 5′ UTR of the zebrafish *igf1rb* gene (including the MO target regions) was generated by RT-PCR (forward primer, 5′-ATCTCGAGAGAACCGCGCTGCTGAGGT-3′; reverse primer: 5′-TAGGATCCTTGCGGAAGACCTCCTGAT-3′). The amplified DNA fragment was digested with *Bam*HI and *Xho*I andesubcloned into the pEGFP-N1 plasmid. The orientation and accuracy of sequences were verified by DNA sequencing.

Microinjection

MOs and/or plasmid DNA were injected into 1–2 cell stage embryos as reported (21). In pilot experiments, control and gene-specific MOs were injected at a range of doses. A nominal concentration of 2.5 ng for each of the two *igf1ra* MOs (5 ng total MO injected per embryo) and 4 ng for each of the two *igf1rb* MOs (8 ng total per embryo) yielded consistent and reproducible phenotypes. These doses were used for all experimental analysis, except for analysis of spontaneous muscle contractility and motoneuron quantification where the same amount of *ifg1ra* MOs and *igf1rb* MOs were injected per embryo (5 ng total MO per embryo). For the GFP reporter assays, 100 pg of plasmid and 2 ng of the indicated MO were injected per embryo.

Western blot

Twenty five embryos from each treatment group were dechorionated, deyolked, and homogenized in 100 μl of RIPA buffer (50 mM Tris-HCl, 150 mM NaCl, 2 mM EGTA, 0.1% Triton X-100, pH 7.5) containing 10 μg/ml aprotinin, 10 μg/ml leupeptin, 10 μg/ml pepstatin, 100 mM PMSF, and 0.1 M sodium orthovanadate. The homogenates were briefly centrifuged to pellet cellular debris and the supernatant was retained. Protein levels of each sample were quantified using a protein assay kit (Pierce Biotechnology, Rockford, IL). Equal amounts of protein were analyzed by SDS-PAGE and Western blot as described previously (22). The total Akt Ab and the phospho-Akt Ab (Ser-473 and Thr308) were both used at a 1:1000 dilution.

Whole mount in situ hybridization and antibody staining

Whole mount *in situ* hybridization using digoxigenin (DIG)-labeled RNA riboprobes and Ab staining were carried out as reported previously (18). Ventricle tissue and skeletal muscle fibers were labeled by F59 staining at 1:10 dilution, hair cells in the otic vesicles were labeled using an anti-Tubulin Ab (1:1000 dilution), and motoneuron axons were labeled by SV2 staining (1:2000 dilution). Microphotographs were taken with a Nikon EC600 fluorescence microscope or acquired by laser scanning confocal microscopy (Model LSM 510, Carl Zeiss, Germany).

Immunocytochemistry

Cryosections were prepared following Hu and Easter et al. (23). The sections (10 μm) were collected and air-dried at

room temperature for 2 h before immunocytochemistry or storage at -20 C. After washing, sections were incubated in PBS at 37 C for 15 min to remove excess gelatin. Nonspecific binding was blocked by incubation in 5% goat serum/0.5% Triton/PBS for 1 h at room temperature. Muscle tissue staining was performed with a 1:20 dilution of F59. The retinal ganglion cell (RGC) layer was immunostained using a 1:500 dilution of Zn5. Primary antibodies were visualized with a 1:500 dilution of a Cy3-conjugated goat antimouse secondary Ab. Nuclei were counterstained with 50 nM sytox (Molecular Probes, Eugene, OR). Images were acquired as described above.

Body size, heart rate, and motoneuron measurements

Body length, somite number, and heart rates were measured as reported (21). The caudal primary motoneurons (CaP) located above the yolk sac extension were quantified in 48 hpf embryos after staining with SV2 followed by color detection using a Vectastain avidin-biotin complex detection kit (Vector Labs; Burlingame, CA). Motoneurons were scored as present regardless of length or organization.

Statistics

Quantitative data are presented as means ± SE. (SEM). Differences among groups were statistically compared using one-way ANOVA followed with PLSD or Student's t test. Statistical significance was accepted when $p < 0.05$.

RESULTS

Genomic structure and chromosomal locations of zebrafish *igf1ra* and *igf1rb*

The genomic structures of zebrafish *igf1ra* and *igf1rb* were determined by searching the zebrafish genome database and PCR. Zebrafish *igf1ra* spans 151.5 kb in the genome. Like the human *IGF1R*, zebrafish *igf1ra* has 21 exons. Zebrafish *igf1rb* spans 156.5 kb in the genome and has an extra exon (#22) in its 3′ end (**Fig. 1*A*, Table 1**). Comparisons of exon lengths of the two zebrafish *igf1r* genes with the human *IGF1R* gene indicated a high degree of cross-species conservation (Table 1). We physically mapped *igf1ra* and *igf1rb* using the LN54 radiation hybrid mapping panel (20). While *igf1rb* mapped to linkage group (LG 7) as previously reported (24), *igf1ra* mapped to zebrafish LG 18 (Fig. 1*B*). Further analysis suggested that *igf1rb* and six other zebrafish genes (*fb50h01, cox5a, herc1, mfap1, p24b* and *gro1*) located on LG 7 have orthologs on human chromosome 15 (**Table 2**) (20, 25–27). Similarly, *igf1ra* and four other zebrafish genes on LG 18 (*arl, fa08a06, mef2a,* and *sema*) also have orthologs on human chromosome 15 (Table 2) (20, 25–27). This result supports existing data that human chromosome 15 shares conserved synteny with zebrafish LGs 7 and 18 (27, 28) and suggests a common ancestry for the human and zebrafish *IGF1R*s.

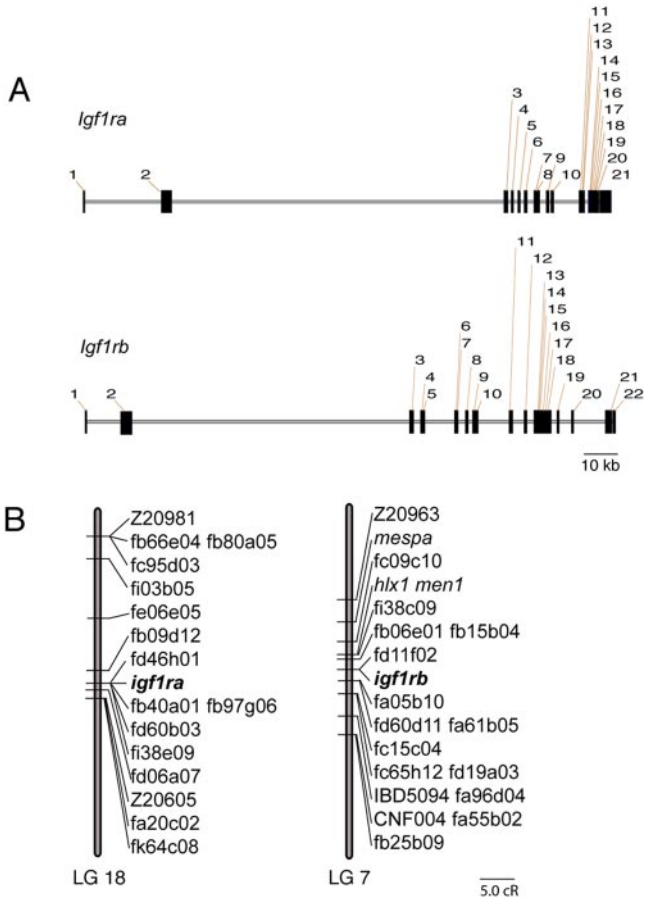

Figure 1. The genomic structure and physical mapping of zebrafish *igf1ra* and *igf1rb*. *A)* A schematic diagram comparing the structures of the zebrafish *igf1ra* and *igf1rb* genes. The horizontal lines represent introns, and the vertical black rectangles represent exons. *B)* Zebrafish *igf1ra* is located on linkage group 18, 2.53 centiRay from marker *fb09d12*, and *igf1rb* is located on linkage group 7, 4.71 centiRay from marker *fc09c10*. 1 centiRay = 148 kb.

Targeted knockdown of zebrafish *igf1ra* and *igf1rb* and inhibition of Igf signaling

To determine the functions of *igf1ra* and *igf1rb*, we ablated each gene product using two independent antisense MOs for each gene. Two gene-specific missense MOs were used as controls. The efficacy and specificity of these MOs in knocking down their respective target gene product were determined using *igf1ra*-GFP and *igf1rb*-GFP, two reporter genes generated by fusing a portion of the 5′UTR of each receptor (containing the MO targeting sequences) upstream of GFP. Injection of either the *igf1ra*-GFP or *igf1rb*-GFP plasmids into zebrafish embryos resulted in mosaic GFP expression (**Fig 2*A***). As shown in Fig. 2*A* and 2B, coinjection of the *igf1ra*-GFP plasmid with either *igf1ra* MO significantly reduced the number of GFP-expressing embryos from 81.40 ± 3.76% in embryos injected with control MOs (n=149), to 1.67 ± 0.58% in embryos injected with *igf1ra* MO 1 (n=143) and 1.33 ± 0.58% in embryos injected with *igf1ra* MO 2 (n=159). In

TABLE 1. *Structural conservation between the human IGF1R and the duplicate zebrafish igf1rs*[a]

Exon number	Exon length		
	Human *IGF1R*	Zebrafish *igf1ra*	Zebrafish *igf1rb*
1	1,042	94	82
2	546	564	531
3	313	**304**	298
4	149	137	*149*
5	145	***145***	***145***
6	215	**209**	**209**
7	127	***127***	***127***
8	239	**236**	254
9	168	***168***	***168***
10	202	**205**	**205**
11	284	**278**	**281**
12	137	**143**	**134**
13	160	**166**	**166**
14	103	***103***	**100**
15	71	***71***	***71***
16	230	**232**	***230***
17	111	**106**	**108**
18	160	**163**	***160***
19	130	**132**	***130***
20	135	**132**	***135***
21	1,000	541	460
22			237

[a]Zebrafish *igf1r* exons in boldface indicate ±10 bp difference in length compared to the human *IGF1R*, and exons in italics are identical in length.

contrast, coinjection of *igf1rb* MO 1 + 2 had no such effect (85.93±1.99%, n=172). Similarly, coinjection of the *igf1rb*-GFP plasmid with either *igf1rb* MO significantly reduced the number of GFP-expressing embryos from 86.0 ± 3.13% in embryos injected with control MOs (n=121), to 3.3 ± 0.47% in embryos injected with *igf1rb* MO 1 (n=94) and 4.5 ± 0.57% in embryos injected with *igf1rb* MO 2 (n=111). Coinjection of *igf1ra* MO 1 + 2 had no such effect (78.7±2.72%, n=94). To show that the endogenous Igf1r-mediated signaling was indeed impaired, we analyzed the levels of Akt phosphorylation. Akt is a major downstream effector of the IGF1R in mammals and in zebrafish (29). Western blot analysis indicated a marked reduction in the levels of phosphorylated Akt in the *igf1r*a and *igf1rb* MO-injected groups compared to controls. There was a further decrease in the group of embryos injected with a combination of *igf1r*a and *igf1rb* MOs. Together, these data indicate that the *igf1r* MOs efficiently and specifically target their respective gene product and disrupt Igf1r-mediated signaling.

Igf1ra and Igf1rb are both required for proper embryonic growth, development, and survival

Embryos injected with control MOs were indistinguishable from wild type embryos (**Fig. 3*A***). In contrast, injection of either *igf1ra* MO 1 or *igf1ra* MO 2 resulted in embryos that were smaller and developmentally delayed (Fig. 3*A*). Likewise, injecting either *igf1rb* MO 1 or *igf1rb* MO 2 caused similar growth and developmental retardation (Fig. 3*A*). Because injecting multiple targeting MOs is known to exert maximal effects (30, 31), we injected both MOs for each receptor. Indeed, these embryos exhibited more severe phenotypes (Fig. 3*A*) and were used for subsequent analysis. All *igf1ra* and *igf1rb* MO-injected embryos survived to 48 hpf and ~50% were alive at 72 hpf but none beyond 96 hpf. At 24 hpf, the mean body lengths of *igf1ra* MO and *igf1rb* MO-injected embryos were 0.95 ± 0.03 mM and 1.00 ± 0.02 mM, respectively (Fig. 3*B*). These values were significantly smaller compared to that of control MO-injected embryos (1.598±0.02 mM). Knockdown of either *igf1ra* or *igf1rb* significantly reduced somite number, which is a quantitative indicator of the developmental rate in zebrafish before 24hpf (19). Compared to 29.97 ± 0.20 somites in control MO-injected embryos, *igf1ra* MO-injected embryos had only 20.14 ± 0.28 somites, and *igf1rb* MO-injected embryos had only 19.54 ± 0.48 somites (Fig. 3*C*). According to this criterion, embryos at 24 hpf in *igf1ra* and *igf1rb* MO-injected groups were developmentally equivalent to control embryos at ~18 hpf. These results indicate that knockdown of either zebrafish *igf1ra* or *igf1rb* resulted in embryonic lethality, growth retardation, and developmental delay.

To determine the effect of ablating both *igf1r* genes simultaneously, we injected a combination of all four targeting MOs. All injected embryos died by 30 hpf. At 24 hpf, their mean body length was 0.854 ± 0.02 mM, significantly smaller than those of the single knockdown group ($P < 0.001$). Likewise, knockdown of *igf1ra* and *igf1rb* together resulted in a further reduction in somite number (16.02±0.31), which is significantly smaller than those of the single knockdown group ($P < 0.001$). These data indicate that Igf1ra and Igf1rb play overlapping but nonredundant roles in regulating embryonic growth, developmental rate, and survival.

TABLE 2. *Comparisons of genes mapped on zebrafish LGs 7 and 18 with those on human chromosome 15*

Human	Zebrafish	Zebrafish
Chr 15	LG 18	LG 7
ALDH6		*fb50h0*[20]
ARL	*arl*[25]	
COX5A		*cox5a*[27]
GATM	*fa08a06*[26]	
HERC1		*herc1*[27]
IGF1R	*igf1ra*[20,26]	*igf1rb*[20,27]
MEF2A	*mef2a*[26,27]	
MFAP1		*mfap1*[27]
p24b		*p24b*[27]
SEMA2	*sema2*[27]	
TLE3		*gro1*[20,27]

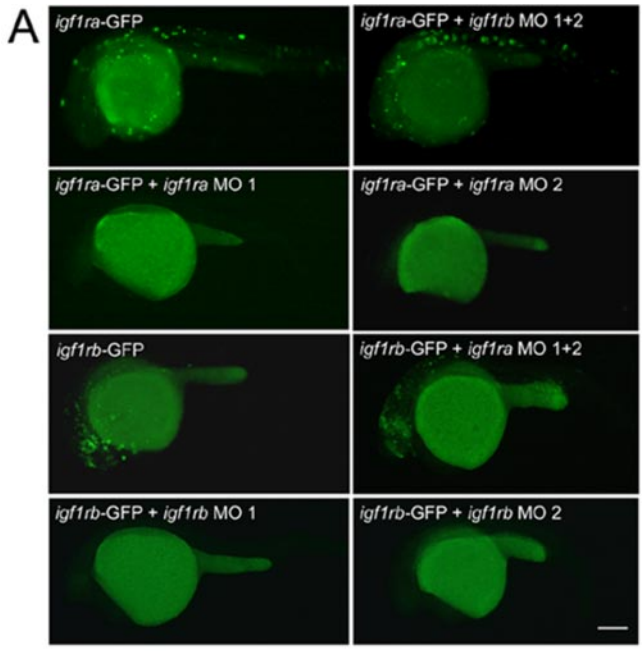

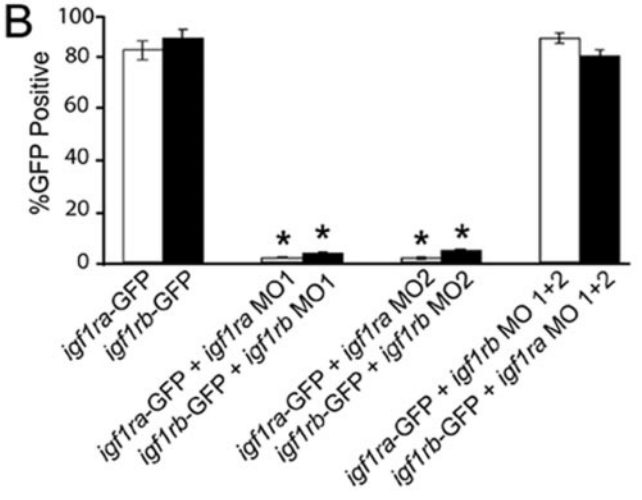

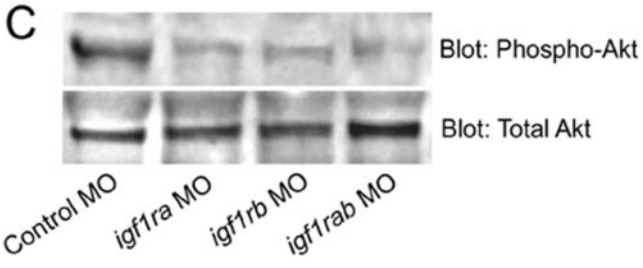

Figure 2. Specific knockdown of *igf1ra* and *igf1rb*. *A)* Fluorescence microscopy images of zebrafish embryos injected with either *igf1ra*-GFP or *igf1rb*-GFP reporter plasmids, with or without *igf1ra* and *igf1rb* MOs. Lateral views are shown with anterior to the left and dorsal up. Each GFP plasmid was injected with or without the indicated MO. The yolk sac is autofluorescent. Scale bar = 250 μm. *B)* Quantification of (*A*). Data are presented as means ± SEM Results were obtained from three independent microinjection experiments, each with at least 30 embryos per group. *, $P < 0.0001$ compared to the control MO-injected group. *C)* Knockdown of *igf1ra* and/or *igf1rb* reduces phosphorylated Akt levels. Embryos injected with either *igf1ra* MOs, *igf1rb* MOs, or *igf1ra* MO and *igf1rb* MOs were subjected to Western blot analysis using antibodies for total and phospho-Akt. Similar results were obtained in two other experiments.

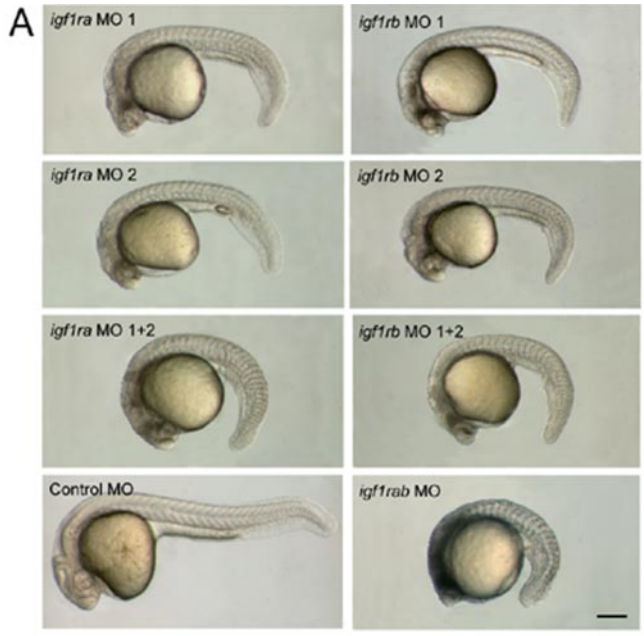

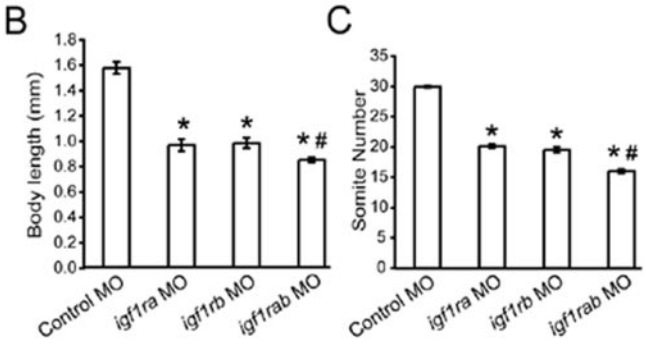

Figure 3. Knockdown of *igf1ra* and/or *igf1rb* reduces embryonic growth and developmental rate. *A)* Morphology of 24 hpf embryos injected with *igf1ra* MO 1, *igf1ra* MO 2, *igf1ra* MO 1 + 2, *igf1rb* MO 1, *igf1rb* MO 2, *igf1rb* MO 1 + 2, all four *igf1r* MOs (*igf1ra*b MO), or control MOs. Scale bar = 250 μm. *B)* Body length and *C)* somite number of embryos injected with either *igf1ra* MOs (*igf1ra* MO 1+MO 2), *igf1rb* MOs (*igf1rb* MO 1+2), *igf1rab* MOs (all four *igf1r* MOs), or control MOs. Results are from three independent microinjection experiments, each with 15 embryos per group. *$P <$ 0.0001 compared with the control MO-injected group, and # $P < 0.001$ compared with that of the *igf1ra* or *igf1rb* MO-injected group.

Overlapping roles of zebrafish Igf1ra and Igf1rb in eye, inner ear, and heart development

To investigate the functional roles of the zebrafish Igf1rs, we analyzed the impact of knocking down *igf1ra* or *igf1rb* on organogenesis of the eye, inner ear, and heart. As shown in **Fig. 4*A***, knockdown of either *igf1ra* or *igf1rb* markedly reduced the expression levels of *rx1*

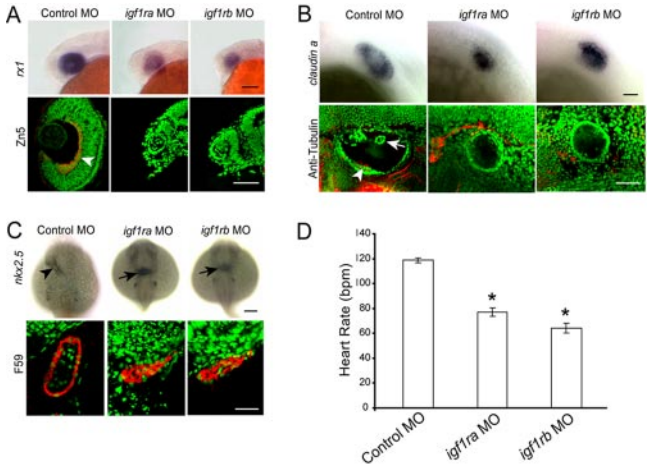

Figure 4. Knockdown of *igf1ra* or *igf1rb* causes similar defects in eye, inner ear, and heart development. *A)* Expression of *rx1* mRNA in 24 hpf embryos injected with control MOs, *igf1ra* MOs, or *igf1rb* MOs (upper panels). Scale bar = 100 μm. Differentiated retinal ganglion cells (red, Zn5 staining, arrowhead) in 48 hpf embryos injected with control MOs, *igf1ra* MOs, or *igf1rb* MOs. The sections were counter stained with sytox (green, nuclear staining). Dorsal views are shown with anterior up. Scale bar = 50 μm. Similar results were obtained in two independent microinjection experiments. *B)* Expression of *claudin a* mRNA in 24 hpf embryos injected with control MOs, *igf1ra* MOs, or *igf1rb* MOs (upper panels). Differentiated hair cells labeled by anti-Tubulin antibody staining (red, arrowhead) in 48 hpf embryos injected with control MOs, *igf1ra* MOs, or *igf1rb* MOs. The sections were counter stained with sytox (green, nuclear staining). Epithelium protrusions (arrow), which mark the beginning of semicircular canal formation, were also absent in *igf1ra* and *igf1rb* MO-injected embryos. Lateral views are shown with anterior to the left and dorsal up. Scale bars = 50 μm. Similar results were obtained in two independent microinjection experiments. *C)* Expression of *nkx2.5* mRNA in 24 hpf embryos injected with control MOs, *igf1ra* MOs, or *igf1rb* MO (upper panels). Note the tubular heart in the control MO-injected embryo (arrowhead), compared to the shallow cone structure of the heart tissue in *igf1ra* and *igf1rb* MO-injected embryos (arrows). Dorsal views are shown with anterior up. Scale bar = 100 μm. Differentiated cardiac cells (red, labeled by F59 staining) in 48 hpf embryos injected with control MOs, *igf1ra* MOs, or *igf1rb* MOs. The sections were counter stained with sytox (green, nuclear staining). Ventricles in *igf1ra* and *igf1rb* MO-injected embryos failed to form distinct chambers. Lateral views are shown with anterior to the left and dorsal up. Scale bar = 50 μm. Similar results were obtained in three independent experiments. *D)* Heart rates (bpm = beat per minute) in 48 hpf embryos injected with control MOs, *igf1ra* MOs or *igf1rb* MOs. Results were obtained from three independent microinjection experiments, each with 15 embryos per group. $*P < 0.001$.

mRNA, a retina-specific homoebox gene. Neurogenesis in the zebrafish retina begins with the differentiation of the retinal ganglion cells (RGCs) at around 30 hpf (32). By 48 hpf, RGC axons occupy the inner layer of the retina and converge to form a single bundle of axons as they pass out of the retina (33, 34). Staining of cryosections of control, *igf1ra,* and *igf1rb* MO-injected embryos at 48 hpf with an RGC-specific antibody (Zn5) revealed a general absence of differentiated RGCs in the retina (Fig. 4*A*). Similarly, there was a notable reduction in the expression domain of *claudin a*, an otic vesicle (inner ear) marker, in *igf1ra* and *igf1rb* MO-injected embryos (Fig. 4*B*). In developing zebrafish otic vesicles, differentiated sensory hair cells are detectable by 36 hpf, and these cells can be labeled by anti-Tubulin staining (35). Analysis of 48 hpf *igf1ra* and *igf1rb* MO-injected embryos revealed a lack of differentiated sensory hair cells (Fig. 4*B*). Additionally, the protrusions in the epithelium, which mark the beginning of semicircular canal formation, were also absent in *igf1ra* and *igf1rb* MO-injected embryos (Fig. 4*B*). Since knockdown of *igf1ra* and *igf1rb* together caused early lethality, these analyses could not be performed in these embryos.

We also detected a delay in heart morphogenesis caused by depleting of Igf1ra or Igf1rb. *In situ* hybridization analysis of *nkx2.5* expression, a heart-specific homeobox gene, indicated that hearts in 24 hpf control MO-injected embryos developed into tubular structures. In contrast, the ventricular tissue in *igf1ra* and *igf1rb* MO-injected embryos remained shallow cones, resembling WT embryos at ~18 hpf. Immunostaining using F59 revealed a notable reduction in heart size in *igf1ra* and *igf1rb* MO-injected embryos (Fig. 4*C*). The ventricles of *igf1ra* and *igf1rb* MO-injected embryos failed to form distinct chambers as observed in control MO-injected embryos. There were also changes in heart function (Fig. 4*D*). While the mean heart rate of control MO-injected embryos was 120.5 ± 1.88 bpm (beats per minute), the heart rates of *igf1ra* and *igf1rb* MO-injected embryos were significantly lower (79.8±9.16 bpm and 72.3±7.51 bpm). Taken together, these results indicated that *igf1ra* and *igf1rb* play largely similar roles in eye, inner ear, and heart development.

Igf1rb plays a greater role in spontaneous muscle contractility and motoneuron development.

During the course of the study, we noticed a marked difference in spontaneous contractile activity among the experimental groups. Wild-type zebrafish embryos spontaneously contract their tail muscles at 24 hpf as their motoneuron axons innervate their somitic myotomes (36). By 48 hpf, this spontaneous contractility ceases and embryos exhibit rhythmic bouts of swimming. Control MO-injected embryos were indistinguishable from their wild-type siblings, 100% exhibiting spontaneous muscle contractions at 24 hpf and 0% at 48 hpf (**Fig. 5*A***). In *igf1ra* MO-injected embryos, 69.0 ± 3.07% of the embryos at 24 hpf and 91.5 ± 0.54% at 48 hpf displayed spontaneous contractility, indicating that depletion of *igf1ra* delayed or prolong the timing of this behavior. In contrast, few of the *igf1rb* MO-injected embryos exhibited spontaneous muscle contractility at either 24 hpf (8.65±0.60%) or 48 hpf (5.5±0.75%), suggesting that depletion of *igf1rb* either abolished this behavior or caused a greater delay.

The lack of spontaneous muscle contractility would imply defects in muscle differentiation, motoneuron

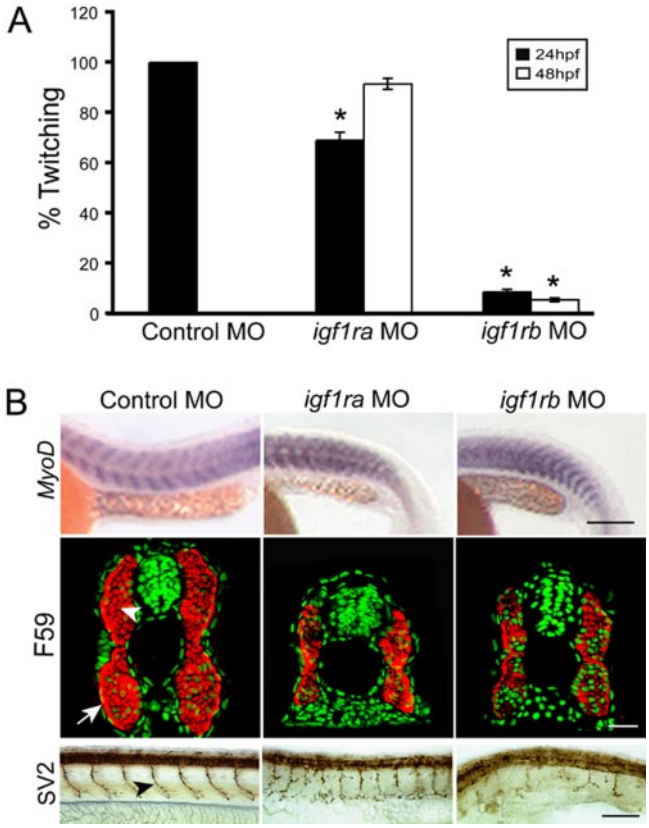

Figure 5. Igf1rb plays a greater role in regulating spontaneous muscle contractility and motoneuron formation. *A)* Percent of embryos exhibiting spontaneous muscle contractility at 24 (filled bar) or 48 hpf (open bar) injected with control MOs, *igf1ra* MOs, or *igf1rb* MOs. Results were obtained from three independent microinjection experiments, with 45 embryos per group. $*P < 0.0001$ between either *igf1ra* or *igf1rb* MO-injected embryos (24 and 48 hpf) and control MO-injected embryos (24hpf). *B)* Expression of *myoD* mRNA in 24 hpf embryos injected with control MOs, *igf1ra* MOs, or *igf1rb* MOs. Scale bar = 250 μm. Differentiated staining slow and fast muscles (labeled by F59 staining, red) of 48 hpf embryos injected with control MOs, *igf1ra* MOs, or *igf1rb* MOs. The sections were counter stained with sytox (green, nuclear staining). Scale bar = 20 μm. Analysis of CaP motoneuron axons in 48 hpf control, *igf1ra,* and *igf1rb* MO-injected embryos stained with anti-SV2, a synaptic vesicle protein expressed in motoneuron axons. Lateral views are shown with anterior to the left and dorsal up. Scale bar = 100 μm. Similar results were obtained in three independent microinjection experiments.

innervation, or both. To determine whether knockdown of *igf1ra* or *igf1rb* caused defects in somite formation, *in situ* hybridization was performed using probes for *myoD* and *myogenin* expression. Both *igf1ra* and *igf1rb* MO-injected embryos showed robust mRNA expression of *myoD* (Fig. 5*B*) and *myogenin* (data not shown) at 24 hpf, indicating no defects in somitogenesis. Immunostaining of 48 hpf embryos using F59 (labeling both fast and slow muscle at this stage) indicated that knockdown of either *igf1ra* or *igf1rb* caused a reduction in differentiated slow and fast muscle. The degree of reduction, however, was comparable (Fig. 5*B*). Therefore, although muscle differentiation was impaired, it is not likely the underlying cause of the difference observed with spontaneous muscle contractility. These results led us to hypothesize alternately that *igf1rb* may perhaps be more important for promoting motoneuron differentiation. To test this idea, 48 hpf old control, *igf1ra,* and *igf1rb* MO-injected embryos were stained with an Ab against SV2, which is a synaptic vesicle membrane protein expressed in motoneurons and their axons. As shown in Fig. 5*B*, axons of CaP motoneurons in control MO-injected embryos clearly innervated the muscle and were well organized, but CaP axons in *igf1ra* and *igf1rb* MO-injected embryos were significantly impaired. In particular, *igf1rb* MO-injected embryos exhibited a reduced number of CaP motoneuron axons. To quantify this effect, we measured the number of CaP axons innervating the somites above the yolk sac extension. There were only 4.5 ± 0.46 axons detected in *igf1rb* MO-injected embryos. This value was significantly less than the 8.4 ± 0.8 axons in *igf1ra* MO-injected embryos ($n=8$, $P<0.0001$), which was comparable to control MO-injected embryos (9.0 ± 0.0 axons). These data suggest that while both *igf1ra* and *igf1rb* are important for muscle differentiation, Igf1rb plays a more specific or greater role in promoting motoneuron innervation.

DISCUSSION

It is well established that IGF1R-mediated signaling is essential for normal organismal survival, growth, and development in mammals (1–4). The accumulated evidence to date suggests that the major components of the Igf signaling system in teleosts are similar to those in mammals (37). However, there are several key differences. During mammalian fetal development, the mannose 6-phosphate/ type 2 Igf receptor (M6P/IGF2R) has an important function as a biological sink to prevent tissue overgrowth stimulated by IGF2 (3). Comparative studies indicate that the mannose 6-phosphate receptors of nonmammalian species do not possess the capacity to bind IGF2 with high-affinity (37). In contrast to the presence of a single *IGF1R* gene in mammals, zebrafish and other teleost species have two genes structurally related to the human *IGF1R* (18, 38). These two receptors are orthologous to the human *IGF1R* gene phylogenetically, and they both bind to IGFs, but not insulin (18). In this study, we provide evidence that zebrafish Igf1ra and Igf1rb are encoded by distinct genetic loci believed to have evolved from a common ancestral locus. There is strong syntenic correspondence between the two zebrafish *igf1r* genes and the human *IGF1R* gene, suggesting that zebrafish *igf1ra* and *igf1rb* originated from a gene duplication event that occurred during teleost evolution. The high degree of conservation in the exon number and length also supports this idea. A previous study has also identified two cDNAs encoding two structurally distinct insulin receptor genes (18). These findings are consistent with the proposal that zebrafish and other ray-

finned fishes may have experienced an additional gene duplication event during evolution, a theory derived from studies of the Hox gene family in zebrafish and *Fugu* (39).

The finding that two *igf1r* genes are present in zebrafish raised the interesting question regarding their functional relationship. Gene duplication is thought to be the primary source of new genes (40) and evolution by gene duplication has emerged as a general principal of biological evolution, evident in a number of sequenced genomes ranging from Bacteria to humans (41). Permanent preservation of both duplicates requires divergent functions, but deciphering whether a pair of duplicated genes has evolved divergent functions is often challenging. The zebrafish is uniquely positioned to provide insight into the process of functional gene evolution due to its versatility, amenability to manipulation, and because it possess a large number of duplicated genes. In this study, we explored the power of the zebrafish model and determined the functional relationship of the duplicated zebrafish *igf1r* genes. Knockdown of zebrafish *igf1ra* and *igf1rb* together resulted in 100% lethality by 30 hpf. These embryos were also significantly smaller in body size, about half that of their wild type siblings. They also had significantly reduced somite number, suggesting delayed temporal development. These phenotypes are consistent with those reported in human patients, *Igf1r* null mice, and insulin receptor mutant *Drosophila* (5, 6, 42), suggesting that the role of IGF1R-mediated signaling in growth, development, and survival is conserved across a wide range of species. When either *igf1ra* or *igf1rb* was knocked down, the embryos could survive beyond 48 hpf, but with greatly increased mortality rates thereafter. Knockdown of *igf1ra* or *igf1rb* individually also resulted in similar growth retarded and developmentally delayed phenotypes. Additionally, knockdown of *igf1ra* or *igf1rb* resulted in a similar reduction of differentiated RGCs, sensory hair cells in the inner ear, and skeletal muscle. Heart development and growth were also impaired in these embryos. These results suggest that the duplicated zebrafish *igf1r* genes play largely overlapping roles in zebrafish development.

Despite these apparent overlapping functions, Igf1ra or Igf1rb are not strictly redundant, but appear to play additive roles, because embryos lacking both receptors are more severely growth and developmentally retarded than embryos lacking either receptor alone. It also appears that Igf1ra and Igf1rb have evolved divergent functions. While knockdown of either *igf1rb* or *igf1ra* caused a comparable reduction in muscle differentiation, knockdown of *igf1rb*, but not *igf1ra*, caused a failure of embryos to exhibit spontaneous muscle contractility. Further analysis indicated that Igf1rb plays a more specific or greater role in promoting motoneuron innervation of the myotome. Two dominant hypotheses have been proposed regarding the rules governing the functional divergence after gene duplication. The neofunctionalization hypothesis argues that after duplication one daughter gene retains the ancestral function while the other acquires new functions (40). The duplication-degeneration-complementation (DDC) hypothesis asserts that the functions of the ancestral gene are partitioned between the duplicated genes, such that the duplicate genes complement each other by jointly performing the necessary subfunctions of the ancestral gene (43). Our findings concerning the functions of the duplicated zebrafish *igf1r* genes cannot yet be adequately explained by either theory, but are more consistent with recent emerging evidence suggesting that neither subfunctionalization nor neofunctionalization alone can explain the functional evolution of duplicated genes. It has been proposed that a large portion of duplicated genes undergo rapid subfunctionalization followed by prolonged and substantial neofunctionalization (44). Therefore, it is possible that both mechanisms governing duplicated gene evolution have contributed to the current functional state of the two distinct zebrafish *igf1r*s.

The mechanism underlying the functional differences in spontaneous muscle contractility and motoneuron maturation/axon extension between zebrafish Igf1ra and Igf1rb is not yet clear. However, there are precedents for two or more isoforms of a growth factor receptor exerting different functions. For example, the two mammalian platelet-derived growth factor (PDGF) receptors (PDGFR), PDGFαR and PDGFβR, are thought to be products of a gene duplication event predating the divergence of nonjawed vertebrates and jawed vertebrates (45, 46). The *PDGFαR* and *PDGFβR* genes exhibit different spatiotemporal expression patterns, and display distinct ligand binding properties. While PDGFαR binds, and is activated by all forms of PDGF (AA, BB and AB), PDGFβR is activated exclusively by PDGF-BB (45, 46). Furthermore, exchanging the intracellular signaling domains of the mouse PDGFαR and PDGFβR, caused differences in the abilities of these chimeric receptors to mediate sustained MAP kinase activation, resulting in varying degrees of vascular disease (45, 47). Differences in ligand binding affinities, gene expression patterns, and/or signal transduction mechanisms may account for the functional specificity of the two zebrafish *igf1r* genes. Previous studies have demonstrated that both zebrafish Igf1ra and Igf1rb bind Igfs and that the two zebrafish genes display similar spatial expression patterns during early development, although there are temporal differences in their relative abundance (18). In particular, higher levels of Igf1rb were observed in early embryonic stages (18). It was also noted that the two zebrafish Igf1rs are only 70% identical to each other, with the divergent residues spread throughout the molecules, and there are significant differences in the cytoplasmic regions of the two Igf1rs. It is possible that these divergent sequences may confer different signaling capacities between the two receptors. Further studies focusing on determining whether the duplicated zebrafish Igf1rs possess similar or different cellular distribution patterns and/or signaling

properties will be needed to elucidate the molecular mechanisms underlying their functions. FJ

This study was supported in part by NSF IBN 0110864 to C.D. We thank Drs. A.W. Wood and J. Zhang for thoughtful comments on earlier drafts of this manuscript. We would also like to thank Drs. M. Ekker, F. Stockdale, R. Kollmar, S. Lyons, P. Raymond, and S.J. Du for kindly providing reagents for this work.

REFERENCES

1. Le Roith, D., Bondy, C., Yakar, S., Liu, J. L., and Butler, A. (2001) The somatomedin hypothesis: 2001. *Endocr. Rev.* **22,** 53–74
2. Jones, J. I., and Clemmons, D. R. (1995) Insulin-like growth factors and their binding proteins: biological actions. *Endocr. Rev.* **16,** 3–34
3. Nakae, J., Kido, Y., and Accili, D. (2001) Distinct and overlapping functions of insulin and IGF-I receptors. *Endocr. Rev.* **22,** 818–835
4. De Meyts, P., and Whittaker, J. (2002) Structural biology of insulin and IGF1 receptors: implications for drug design. *Nat. Rev. Drug Discov.* **1,** 769–783
5. Abuzzahab, M. J., Schneider, A., Goddard, A., Grigorescu, F., Lautier, C., Keller, E., Kiess, W., Klammt, J., Kratzsch, J., Osgood, D., Pfaffle, R., Raile, K., Seidel, B., Smith, R. J., and Chernausek, S. D. (2003) IGF-I receptor mutations resulting in intrauterine and postnatal growth retardation. *N. Engl. J. Med.* **349,** 2211–2222
6. Kawashima, Y., Kanzaki, S., Yang, F., Kinoshita, T., Hanaki, K., Nagaishi, J., Ohtsuka, Y., Hisatome, I., Ninomoya, H., Nanba, E., Fukushima, T., and Takahashi, S. (2005) Mutation at cleavage site of insulin-like growth factor receptor in a short- stature child born with intrauterine growth retardation. *J. Clin. Endocr. Metab.* **90,** 4679–4687
7. Woods, K. A., Camacho-Hubner, C., Savage, M. O., and Clark, A. J. (1996) Intrauterine growth retardation and postnatal growth failure associated with deletion of the insulin-like growth factor I gene. *N. Engl. J. Med.* **335,** 1363–1367
8. Denley, A., Wang, C. C., McNeil, K. A., Walenkamp, M. J., van Duyvenvoorde, H., Wit, J. M., Wallace, J. C., Norton, R. S., Karperien, M., and Forbes, B. E. (2005) Structural and functional characteristics of the Val44Met insulin-like growth factor I missense mutation: correlation with effects on growth and development. *Mol. Endocrinol.* **19,** 711–721
9. Walenkamp, M. J., Karperien, M., Pereira, A. M., Hilhorst-Hofstee, Y., van Doorn, J., Chen, J. W., Mohan, S., Denley, A., Forbes, B., van Duyvenvoorde, H. A., van Thiel, S. W., Sluimers, C. A., Bax, J. J., de Laat, J. A., Breuning, M. B., Romijn, J. A., and Wit, J. M. (2005) Homozygous and heterozygous expression of a novel insulin-like growth factor-I mutation. *J. Clin. Endocrinol. Metab.* **90,** 2855–2864
10. Baker, J., Liu, J. P., Robertson, E. J., and Efstratiadis, A. (1993) Role of insulin-like growth factors in embryonic and postnatal growth. *Cell* **75,** 73–82
11. Liu, J. P., Baker, J., Perkins, A. S., Robertson, E. J., and Efstratiadis, A. (1993) Mice carrying null mutations of the genes encoding insulin-like growth factor I (Igf-1) and type 1 IGF receptor (Igf1r). *Cell* **75,** 59–72
12. Efstratiadis, A. (1998) Genetics of mouse growth. *Int. J. Dev. Biol.* **42,** 955–976
13. Kim, J. J., and Accili, D. (2002) Signalling through IGF-I and insulin receptors: where is the specificity? *Growth Horm. IGF Res.* **12,** 84–90
14. Pera, E. M., Ikeda, A., Eivers, E., and De Robertis, E. M. (2003) Integration of IGF, FGF, and anti-BMP signals via Smad1 phosphorylation in neural induction. *Genes Dev.* **17,** 3023–3028
15. Pera, E. M., Wessely, O., Li, S. Y., and De Robertis, E. M. (2001) Neural and head induction by insulin-like growth factor signals. *Dev. Cell* **1,** 655–665
16. Richard-Parpaillon, L., Heligon, C., Chesnel, F., Boujard, D., and Philpott, A. (2002) The IGF pathway regulates head formation by inhibiting Wnt signaling in Xenopus. *Dev. Biol.* **244,** 407–417
17. Eivers, E., McCarthy, K., Glynn, C., Nolan, C. M., and Byrnes, L. (2004) Insulin-like growth factor (IGF) signalling is required for early dorso-anterior development of the zebrafish embryo. *Int. J. Dev. Biol.* **48,** 1131–1140
18. Maures, T., Chan, S. J., Xu, B., Sun, H., Ding, J., and Duan, C. (2002) Structural, biochemical, and expression analysis of two distinct insulin-like growth factor I receptors and their ligands in zebrafish. *Endocrinology* **143,** 1858–1871
19. Kimmel, C. B., Ballard, W. W., Kimmel, S. R., Ullmann, B., and Schilling, T. F. (1995) Stages of embryonic development of the zebrafish. *Dev. Dyn.* **203,** 253–310
20. Hukriede, N. A., Joly, L., Tsang, M., Miles, J., Tellis, P., Epstein, J. A., Barbazuk, W. B., Li, F. N., Paw, B., Postlethwait, J. H., Hudson, T. J., Zon, L. I., McPherson, J. D., Chevrette, M., Dawid, I. B., Johnson, S. L., and Ekker, M. (1999) Radiation hybrid mapping of the zebrafish genome. *Proc. Natl. Acad. Sci. U. S. A.* **96,** 9745–9750
21. Wood, A. W., Schlueter, P. J., and Duan, C. (2005) Targeted knockdown of insulin-like growth factor binding protein-2 disrupts cardiovascular development in zebrafish embryos. *Mol. Endocrinol.* **19,** 1024–1034
22. Duan, C., Ding, J., Li, Q., Tsai, W., and Pozios, K. (1999) Insulin-like growth factor binding protein 2 is a growth inhibitory protein conserved in zebrafish. *Proc. Natl. Acad. Sci. U. S. A.* **96,** 15274–15279
23. Hu, M., and Easter, S. S. (1999) Retinal neurogenesis: the formation of the initial central patch of postmitotic cells. *Dev. Biol.* **207,** 309–321
24. Ayaso, E., Nolan, C. M., and Byrnes, L. (2002) Zebrafish insulin-like growth factor-I receptor: molecular cloning and developmental expression. *Mol. Cell. Endocrinol.* **191,** 137–148
25. Gates, M. A., Kim, L., Egan, E. S., Cardozo, T., Sirotkin, H. I., Dougan, S. T., Lashkari, D., Abagyan, R., Schier, A. F., and Talbot, W. S. (1999) A genetic linkage map for zebrafish: comparative analysis and localization of genes and expressed sequences. *Genome Res.* **9,** 334–347
26. Geisler, R., Rauch, G. J., Baier, H., van Bebber, F., Bross, L., Dekens, M. P., Finger, K., Fricke, C., Gates, M. A., Geiger, H., Geiger-Rudolph, S., et al. (1999) A radiation hybrid map of the zebrafish genome. *Nat. Genet.* **23,** 86–89
27. Woods, I. G., Kelly, P. D., Chu, F., Ngo-Hazelett, P., Yan, Y. L., Huang, H., Postlethwait, J. H., and Talbot, W. S. (2000) A comparative map of the zebrafish genome. *Genome Res.* **10,** 1903–1914
28. Barbazuk, W. B., Korf, I., Kadavi, C., Heyen, J., Tate, S., Wun, E., Bedell, J. A., McPherson, J. D., and Johnson, S. L. (2000) The syntenic relationship of the zebrafish and human genomes. *Genome Res.* **10,** 1351–1358
29. Pozios, K.C., Ding, J., Degger, B., Upton, Z., and Duan, C. (2001) IGFs stimulate zebrafish cell proliferation through activating the MAP kinase and PI3-kinase signaling pathways. *Am. J. Physiol.* **280,** R1230–R1239
30. Ekker, S. C. (2000) Morphants: a new systematic vertebrate functional genomics approach. *Yeast* **17,** 302–306
31. Ekker, S. C., and Larson, J. D. (2001) Morphant technology in model developmental systems. *Genesis* **30,** 89–93
32. Neumann, C. J., and Nuesslein-Volhard, C. (2000) Patterning of the zebrafish retina by a wave of sonic hedgehog activity. *Science* **289,** 2137–2139
33. Easter, S. S., Jr., and Malicki, J. J. (2002) The zebrafish eye: developmental and genetic analysis. *Results Probl. Cell Differ.* **40,** 346–370
34. Neumann, C. J. (2001) Pattern formation in the zebrafish retina. *Semin. Cell Dev. Biol.* **12,** 485–490
35. Whitfield, T. T., Riley, B. B., Chiang, M. Y., and Phillips, B. (2002) Development of the zebrafish inner ear. *Dev. Dyn.* **223,** 427–458
36. Drapeau, P., Saint-Amant, L., Buss, R. R., Chong, M., McDearmid, J. R., and Brustein, E. (2002) Development of the locomotor network in zebrafish. *Prog. Neurobiol.* **68,** 85–111
37. Wood, A. W., Duan, C., and Bern, H. A. (2005) Insulin-like growth factor signaling in fish. *Int. Rev. Cytol.* **243,** 215–285
38. Chan, S. J., Plisetskaya, E. M., Urbinati, E., Jin, Y., and Steiner, D. F. (1997) Expression of multiple insulin and insulin-like growth factor receptor genes in salmon gill cartilage. *Proc. Natl. Acad. Sci. U. S. A.* **94,** 12446–12451

39. Amores, A., Force, A., Yan, Y. L., Joly, L., Amemiya, C., Fritz, A., Ho, R. K., Langeland, J., Prince, V., Wang, Y. L., Westerfield, M., Ekker, M., and Postlethwait, J. H. (1998) Zebrafish hox clusters and vertebrate genome evolution. *Science* **282,** 1711–1714
40. Ohno, S. (1970) Evolution by Gene Duplication. *Springer-Verlag, New York*
41. Zhang, J. (2003) Evolution by gene duplication: an update. *Trends Ecol. Evol.* **16,** 292–298
42. Chen, C., Jack, J., and Garofalo, R. S. (1996) The Drosophila insulin receptor is required for normal growth. *Endocrinology* **137,** 846–856
43. Force, A., Lynch, M., Pickett, F. B., Amores, A., Yan, Y. L., and Postlethwait, J. (1999) Preservation of duplicate genes by complementary, degenerative mutations. *Genetics* **151,** 1531–1545
44. He, X., and Zhang, J. (2005) Rapid subfunctionalization accompanied by prolonged and substantial neofunctionalization in duplicate gene evolution. *Genetics* **169,** 1157–1164
45. Klinghoffer, R. A., Mueting-Nelsen, P. F., Faerman, A., Shani, M., and Soriano, P. (2001) The two PDGF receptors maintain conserved signaling in vivo despite divergent embryological functions. *Mol. Cell.* **7,** 343–354
46. Heldin, C. H., Ostman, A., and Ronnstrand, L. (1998) Signal transduction via platelet-derived growth factor receptors. *Biochim. Biophys. Acta* **1378,** F79–113
47. Klinghoffer, R. A., Hamilton, T. G., Hoch, R., and Soriano, P. (2002) An allelic series at the PDGFalphaR locus indicates unequal contributions of distinct signaling pathways during development. *Dev. Cell* **2,** 103–113

Received for publication November 15, 2005.
Accepted for publication January 9, 2006.